Chemistry–A European Journal
Full Paper
doi.org/10.1002/chem.202002879
Chemistry Europe
European Chemical Societies Publishing

Supramolecular Polymers

Impact of Molecular Size and Shape on the Supramolecular Co-Assembly of Chiral Tricarboxamides: A Comparative Study

Yeray Dorca[+],[a] Roberto Sánchez-Naya,[a] Jesús Cerdá[+],[b] Joaquín Calbo,[b] Juan Aragó,[b] Rafael Gómez,[a] Enrique Ortí,*[b] and Luis Sánchez*[a]

Abstract: A comparative investigation of the chiral amplification features of a series of three families of C_3-symmetric tricarboxamides, 1,3,5-triphenylbenzenetricarboxamides (TPBAs), benzenetricarboxamides (BTAs) and oligo(phenylene ethynylene) tricarboxamides (OPE-TAs), is here reported. As previously observed for BTAs and OPE-TAs, a similar dichroic response is obtained for TPBAs decorated with one, two or three chiral side chains bearing stereogenic centers, thus confirming the efficient transfer of point chirality to the supramolecular helical aggregates. Unlike BTAs and OPE-TAs, the chiral amplification ability of TPBAs in majority rules experiments shows a negligible dependence on the number of chiral centers per monomeric unit, and stands the largest among the series of tricarboxamides. Detailed experimental and theoretical studies demonstrate that the rotation angle between the TPBA units in the helical stack is intermediate to that observed for BTAs and OPE-TAs. This feature strongly conditions the steric interactions between vicinal molecules in the stack and the final chiral amplification outcome. Furthermore, theoretical calculations show that achiral side chains favor the interdigitation of the helical aggregates and thereby the formation of bundle superstructures.

Introduction

Chiral amplification, a natural phenomenon by which enantioenriched compounds are generated by the action of a chiral bias, is a topic of broad interest in life sciences.[1] The seminal reports of Green and co-workers on the chiral amplification experienced by achiral polyisocyanates upon the addition of a minute amount of a chiral congener, termed as "sergeants-and-soldiers" (SaS) experiments,[2] or upon mixing unequal amounts of two enantioenriched polyisocyanates, known as "majority rules" (MRs) experiments,[3] paved the way to the application of macromolecules and supramolecular systems in asymmetric catalysis,[4] chiral recognition[5] and circularly polarized luminescence (CPL) emitting materials.[6] To elucidate the principles governing the chiral amplification phenomenon, supramolecular polymers, that is, macromolecular species constituted by the interaction of self-assembling units by noncovalent forces, constitute an excellent benchmark to construct helical aggregates.[7] Scaffolds like merocyanines,[8] naphthalene bisimides,[9] perylene bisimides,[10] or other π-conjugated systems[11] exemplify the variety of moieties investigated for processes of transfer and amplification of chirality. C_3-symmetric systems like triarylamines are especially relevant in the investigation of chiral amplification, because they readily self-assemble into helical aggregates[12] and, in addition, constitute outstanding platforms to expand the knowledge about kinetically controlled supramolecular polymerizations.[13]

The establishment of structure–function rules in the field of chiral amplification is a complex process that requires a thorough understanding of the thermodynamic equilibrium affording enantioenriched samples. This requisite is fulfilled by a large variety of supramolecular polymers that are formed following isodesmic or (anti)cooperative mechanisms and can be easily characterized by their corresponding thermodynamic parameters.[14] In this regard, the different mathematical models utilized for deriving those thermodynamic parameters allows calculating the corresponding nucleation (ΔH_n) and elongation (ΔH_e) enthalpies, the entropy (ΔS), the nucleation (K_n) and elongation (K_e) binding constants, and the cooperativity factor (σ), defined as the quotient K_n/K_e.[15] However, both SaS and MRs experiments imply the mixture of two components and, therefore, are examples of supramolecular co-assembly.[16] Consequently, additional thermodynamic parameters, associated to this supramolecular copolymerization must be taken into account. In particular, the mismatch penalty (MMP) should be considered when studying the supramolecular copolymerization of two different enantiomers. The MMP parameter quantifies the stability decrease of the mixture due to the incorporation of a chiral monomer into an aggregate of its unpreferred helicity in comparison to the separated components.[17,18] The

[a] Y. Dorca,[+] R. Sánchez-Naya, Dr. R. Gómez, Prof. Dr. L. Sánchez
Departamento de Química Orgánica, Facultad de Ciencias Químicas
Universidad Complutense de Madrid
28040 Madrid (Spain)
E-mail: lusamar@ucm.es

[b] J. Cerdá,[+] Dr. J. Calbo, Dr. J. Aragó, Prof. Dr. E. Ortí
Instituto de Ciencia Molecular (ICMol), Universidad de Valencia
c/Catedrático José Beltrán, 2 46980 Paterna (Spain)
E-mail: enrique.orti@uv.es

[+] These authors contributed equally to this work.

Supporting information and the ORCID identification number(s) for the author(s) of this article can be found under: https://doi.org/10.1002/chem.202002879.

balance between MMP and the enthalpy gain experienced by the system upon the formation of the corresponding supramolecular polymer bias the final helical outcome of the co-assembly. Importantly, despite the interest in elucidating the energetic parameters to design efficient chiral co-assemblies and the large number of supramolecular polymers exhibiting chiral amplification, very few reports quantify the helical reversal penalty (HRP) and/or MMP parameters.[17–19] Indeed, examples in which self-assembling units with similar shape and identical noncovalent forces operating in the supramolecular copolymerization are compared in terms of chiral amplification are very scarce. In fact, to the best of our knowledge, this comparative study has only been developed for 1,3,5-benzenetricarboxamides (BTAs) and oligo(phenylene ethynylene) tricarboxamides (OPE-TAs) (Figure 1).[20] In that study, experimental evidence and theoretical calculations demonstrated that the ability of OPE-TAs to induce chiral amplification is lower than that reported for comparatively smaller BTAs. Furthermore, the effect that temperature has on chiral amplification is found to work in opposite directions in these two self-assembling systems. Whilst in BTAs a slight increase in temperature favors chiral amplification, the opposite effect is observed for OPE-TAs.[20]

In an attempt to broaden the scope of previous studies and to elaborate a more accurate structure–function relationship in chiral supramolecular co-assemblies, we report herein a detailed mechanistic study on the chiral amplification experienced by 1,3,5-triphenylbenzenetricarboxamides (TPBAs) endowed with a variable number of chiral side chains (compounds **1**–**2** in Figure 1 a). TBPAs have a molecular size intermediate between that of BTAs and OPE-TAs (Figure 1 b). In a previous work, the hierarchy of asymmetry elements operating in the formation of right- or left-handed helical supramolecular polymers by the C_3-symmetric achiral **3** as well as chiral **1 a** and **2 a** TPBAs was thoroughly investigated.[21]

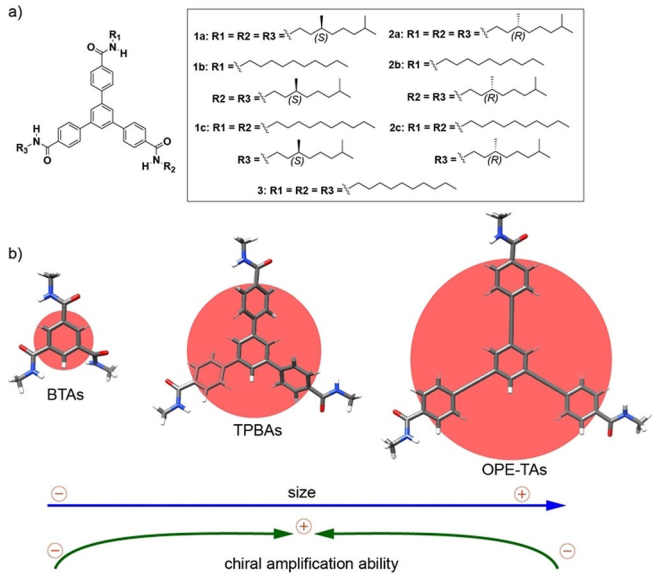

Figure 1. a) Chemical structure of TPBAs **1**–**3**. b) Schematic illustration of the size and chiral amplification ability of TPBAs in comparison to previously reported BTAs and OPE-TAs.

In the present work, only MRs experiments have been performed due to the strong tendency of TPBAs decorated with achiral side chains to bundle into thick fibers.[21] This prevents the completion of reliable SaS experiments because the circular dichroism (CD) response is strongly contaminated by linear dichroism (LD).[22] A complete set of thermodynamic parameters has been derived for all the new self-assembling TPBAs **1**–**2** by applying the equilibrium (EQ) model for one-component systems.[15a] Utilizing this set of parameters, the MMP (ΔH_{mm}) parameter for the mixtures of two enantiomers has been estimated at different temperatures. The thermodynamic analysis shows that MMP remains practically unaltered by modifying the number of stereogenic centers per monomeric unit. This behavior contrasts with that reported for both BTAs and OPE-TAs (Figure 1 b). In the former, the smaller the number of stereogenic centers per monomeric unit, the larger the chiral amplification ability.[18b,c] In the latter, the trend is the opposite, and decreasing the number of stereogenic centers per monomeric unit leads to a smaller chiral amplification.[20] In addition, we have also demonstrated that temperature exerts a weak influence on the chiral amplification ability of the reported TPBAs. Theoretical calculations show that the rotation angle between the TPBA units in a helical stack, which strongly conditions the final chiral amplification outcome for TPBAs, is intermediate between that observed for BTAs and OPE-TAs. The results presented in this manuscript confirm the strong dependence of the chiral amplification ability of self-assembling units on structural factors, like shape and size, and contribute to establish a clear structure–function relationship in chiral supramolecular co-polymers.

Results and Discussion

Synthesis and supramolecular polymerization in solution.

The asymmetric TPBAs **1 b,c** and **2 b,c** were readily prepared in a four-step synthetic protocol involving the amidation of commercially available 4-carboxyphenylboronic acid with the corresponding chiral or achiral amines to yield the 4-(alkylcarbamoyl)phenyl boronic acids **4**. These boronic acids were stoichiometrically reacted with 1,3,5-tribromobenzene in a Suzuki cross-coupling reaction to afford the monoamides **5** that, upon a final Suzuki cross-coupling reaction, yielded the final asymmetric tricarboxamides **1 b,c** and **2 b,c** (Scheme S1). All the new reported compounds were fully characterized by NMR and FTIR spectroscopy as well as by high-resolution mass spectrometry (see the Supporting Information).

As in the case of the previously reported C_3-symmetric TPBAs,[21] and also the referable BTAs and OPE-TAs,[20] ^{1}H NMR and FTIR experiments demonstrate that the self-assembly of the new asymmetric TPBAs **1** and **2** proceeds through the formation of a triple array of H-bonding interactions between the amide functional groups and the π-stacking of the triphenylbenzene (TPB) moieties. Thus, concentration-dependent ^{1}H NMR spectra show the downfield shift of the signal due to the N–H protons and the concomitant shield of the aromatic resonances upon increasing the concentration (Figures S1 and

S2). The operation of N–H···O=C H-bonds between the amides is confirmed by the N–H and amide I stretching vibrational bands. These bands are observed at 3304 and 1633 cm^{-1}, respectively, in a mixture of methylcyclohexane (MCH) and 1,2-dichloroethane (DCE) 95:5,[23] and shift to higher wavenumbers (3452 and 1653 cm^{-1}) in chloroform due to the disassembly in this good solvent (Figure S3).[24] The formation of face-to-face aggregates by the π-stacking of the aromatic TPB units is corroborated by the intensity drop experienced by the broad band at 270 nm observed in the UV/Vis spectra upon cooling (Figure S4).[25]

The presence of stereogenic centers at the peripheral side chains results in an efficient transfer of point chirality from those peripheral chains to the supramolecular chirality involving the aromatic TPB core. This transfer is evidenced by the clear bisignated Cotton effect that diluted solutions of TPBAs **1b** and **2b** exhibit in a 95:5 MCH/DCE mixture at total concentration (c_T) of 10 μM (Figure 2a), diagnostic of the formation of helical structures. The CD spectra of **1b** and **2b**, bearing *S*- and *R*-stereogenic centers, respectively, present mirror-image intense bands at 280 and 259 nm and a zero-crossing point at 270 nm. These features coincide with those previously reported for the C_3-symmetric TPBAs **1a** and **2a**,[21] and demonstrate the generation of helices of opposite handedness, *P*-type for **1b** and *M*-type for **2b**.[26] The dichroic pattern is completely cancelled upon increasing the temperature

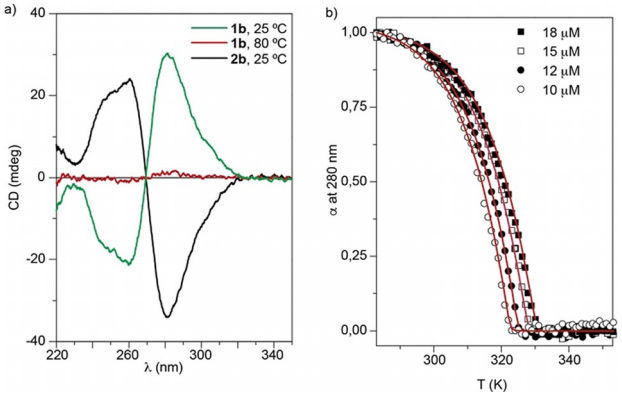

Figure 2. a) CD spectra of TPBs **1b** and **2b** (MCH/DCE, 95:5). b) Plot of the variation of the degree of aggregation, α, versus temperature for **1b** at different concentrations (MCH/DCE, 95:5; cooling rate 1 K min^{-1}). The red lines depict the fitting to the one-component EQ model.

(Figure 2a), which has been employed to determine the supramolecular polymerization mechanism and, by applying the one-component equilibrium (EQ) model,[15a] to derive all the thermodynamic parameters associated to the self-assembly of TPBAs. Plotting the degree of aggregation, α, versus temperature yields non-sigmoidal curves characteristic of cooperative supramolecular polymerizations (Figure 2b and Figure S5).[14] By applying the one-component EQ model, ΔH_n, ΔH_e, ΔS, K_n, K_e, and the cooperativity factor σ were estimated and the respective values are collected in Table 1. The enthalpy and entropy values are comparable to those registered previously for C_3-symmetric **1a** and **2a** (Table 1) but lower than those derived for both BTAs and OPE-TAs. However, the cooperativity factor σ is very similar for all the C_3-symmetric systems.[18e, 20, 21]

Interestingly, the dichroic features of TPBs **1c** and **2c**, endowed with two achiral and one chiral side chains, differ from those obtained for **1b** and **2b** in the same experimental conditions. Freshly prepared solutions of **1c** and **2c** (MCH/DCE 95:5, $c_T = 10$ μM) display bisignate CD spectra with maxima at 237 and 274 nm and a weaker band at 304 nm, with two zero-crossing points at 260 and 295 nm (Figure S6a). The corresponding LD spectra for these solutions showed the presence of a broad band centered around 260 nm (Figure S6b). Therefore, the dissimilar CD spectra of **1c** and **2c** in comparison to TPBAs **1a, 1b, 2a**, and **2b** is justified by the contamination of the CD spectra by the LD effect in the former.[22] To circumvent this problem, we applied a heating/cooling (h/c) cycle (heating up the solutions of **1c** and **2c** to 80 °C and cooling them down to 20 °C) before recording the CD spectra. The application of the h/c cycle cancels the LD contamination, and clean bisignate CD spectra, with intense bands at 280 and 259 nm and a zero-crossing point at 270 nm, identical to those registered for **1a**, **1b**, **2a**, and **2b**, are observed (Figures S6c and S6d). The contamination of the CD spectra with the LD effect has also consequences in the derivation of the thermodynamic parameters. Thus, to achieve cooling curves suitable to apply the EQ model, a rapid cooling (8 K min^{-1}) is needed. This rapid cooling results in a smaller number of data and, consequently, in a less accurate fitting, as indicated by the plots of α vs. temperature (Figure S7) and the significantly different values inferred for the thermodynamic parameters (Table 1). The contamination of the CD response by LD can be accounted for by considering the strong tendency of TPBAs to efficiently interdigitate by van der Waals interactions between the achiral side

Table 1. Thermodynamic parameters derived for the supramolecular polymerization of compounds **1a–c** and **2a–c** (MCH/DCE, 95:5).

	1a[b]	**2a**[b]	**1b**	**2b**	**1c**	**2c**
ΔH_e [kJ mol^{-1}]	−58.8 ± 0.7	−58.1 ± 0.9	−59.9 ± 0.3	−66.9 ± 1.1	−84.2 ± 1.2	−87.9 ± 1.0
ΔS [J K^{-1} mol^{-1}]	−84 ± 2	−82 ± 2	−77 ± 1	−111 ± 1	−166 ± 5	−179 ± 6
ΔH_n [kJ mol^{-1}]	−33 ± 4	−32 ± 6	−28.1 ± 1.4	−29 ± 2	−15.2 ± 1.1	−20.3 ± 1.3
σ[a]	3.0×10^{-6}	2.33×10^{-6}	1.2×10^{-5}	6.8×10^{-6}	2.2×10^{-3}	2.5×10^{-4}
K_e [L mol^{-1}][a]	8.4×10^{5}	8.2×10^{5}	9.2×10^{5}	8.7×10^{5}	1.2×10^{6}	1.1×10^{6}
K_n [L mol^{-1}][a]	2.5	1.9	1.1	5.9	2.7×10^{3}	2.7×10^{2}

[a] The equilibrium constants for elongation and dimerization, K_e and K_n, and the cooperativity factor σ ($=K_n/K_e$) are calculated at 293 K. [b] Data extracted from ref. [21], shown for comparison.

chains, as recently reported for **3**.[21] In the case of **1c** and **2c**, the presence of two achiral side chains favors this bundling effect that results in the formation of larger aggregates (see below) and in the appearance of the LD contribution.

Chiral amplification in asymmetric TPBAs: MRs experiments.

As stated before, SaS experiments were discarded to evaluate the influence of the number of stereogenic centers per monomeric unit on the chiral amplification ability of asymmetric TPBAs **1b**, **2b**, **1c**, and **2c**. The strong tendency of the achiral TPBA **3** to bundle impedes an accurate determination of the CD response when mixing with its chiral congeners owing to the strong contamination by the LD effect.[21] Therefore, we have evaluated the chiral amplification ability of TPBAs by performing MRs experiments. Our previous report on C_3-symmetric chiral **1a** and **2a** demonstrated that in the co-assembly of these two chiral compounds, only a 22% of enantiomeric excess (*ee*) is enough to achieve homochiral mixtures, the MMP being of only 1.0 kJ mol^{-1}.[21] This MMP value is a half of that reported for BTAs (2.1 kJ mol^{-1})[18d] and OPE-TAs (2.0 kJ mol^{-1}).[18b–d,20] Importantly, the values reported for BTAs, and also for OPE-TAs, were obtained for solutions with c_T = 10 μM but those reported for symmetric TBPAs **1a** and **2a** were registered at c_T = 25 μM. To homogenize all the experimental data in a useful way to perform a comparative study, MRs experiments with **1a** and **2a** were conducted also at c_T = 10 μM. In good analogy to the previous MRs study, the derived MMP parameter for 10 μM solutions at 20 °C is 1.4 kJ mol^{-1} (Table 2).

To evaluate the influence of the chiral content per monomeric unit on the ability to induce chiral amplification, we performed MRs experiments by mixing TPBAs **1b** and **2b**, endowed with two (*S*) and two (*R*) stereogenic centers, respectively, and TPBAs **1c** and **2c**, endowed with one (*S*) or (*R*) stereogenic center, respectively. In all these experiments, a nonlinear variation of the dichroic response is observed upon increasing the *ee*, which is a clear indication of an efficient chiral amplification (Figures 3 and Figure S8).

As previously described for BTAs and OPE-TAs,[18b,c,20] decreasing the number of stereogenic centers per monomeric unit in TPBAs also produces a slight decrease of the dichroic response (Figure 3). However, unlike that reported for BTAs and OPE-TAs,[18b,c,20] the ability to induce chiral amplification is found to be practically identical for chiral TPBAs decorated with three (**1a** and **2a**), two (**1b** and **2b**), or one (**1c** and **2c**) stereogenic centers per monomeric unit. In the three TPBA derivatives, an *ee* of ≈20% is enough to achieve homochiral **1a+2a**, **1b+2b**, or **1c+2c** mixtures (Figure 3). This result contrasts with those previously reported for C_3-symmetric tricarboxamides in which *ee* values of 35% and 48% were respectively required for BTAs and OPE-TAs bearing three stereogenic centers to achieve complete amplified states.[18b,c,20] The lower *ee* required to achieve homochiral mixtures in TPBAs in comparison to BTAs and OPE-TAs is justified by the smaller MMP. In addition, for the TPBA systems described herein, the number of stereogenic centers in each self-assembling unit exerts a negligible influence on the chiral amplification ability. This behavior differs from that observed for BTAs, in which the larger the number of stereogenic centers per monomeric unit, the lower the ability for chiral amplification,[18b,c] and also from that exhibited by OPE-TAs, in which the larger the number of stereogenic centers per monomeric unit, the larger the ability for chiral amplification.[20]

To provide a quantitative analysis of the energetics supporting the chiral amplification in TPBAs, the non-linear variation of the dichroic signal upon modifying the *ee* was fitted to the two-components EQ model, which allows deriving the MMP (Figure S9).[15a] The MMP parameter estimated at 20 °C for the investigated mixtures of chiral TPBAs **1** and **2** lies around 1.5 kJ mol^{-1} regardless the number of stereogenic centers per monomeric unit (Table 2). The negligible variation of the MMP value obtained in TPBAs contrasts with that described for BTAs, for which the MMP value at 20 °C decreases from 2.1 to 1.0 kJ mol^{-1} upon decreasing the number of stereogenic centers per monomeric unit.[18b,c] The trend observed for TPBAs is also different to that described for OPE-TAs, for which the MMP increases from 2.0 to 5.4 kJ mol^{-1} at 20 °C upon decreasing the number of stereogenic centers.[20] On the other hand, the low MMP values inferred for TPBAs indicate that the stability of the homochiral mixture of the two enantiomers, due to the incorporation of the enantiomer to the helical aggregate of its unpreferred helicity, is only slightly reduced in comparison to that of the separated components.[16]

In addition to the number of stereogenic centers located on the peripheral side chains of the self-assembling units, temperature also plays a pivotal role in the chiral amplification ability of tricarboxamides. Thus, increasing the temperature results in an increase of the ability of BTAs, quantified by a smaller MMP (from 2.0 kJ mol^{-1} at 20 °C to 1.5 kJ mol^{-1}, at 40 °C, for the BTA with three stereogenic centers).[18b] In contrast, high temperatures increase the MMP value in OPE-TAs (between 2.0 kJ mol^{-1} at 20 °C to 3.3 kJ mol^{-1} at 40 °C, for the OPE-TA with three stereogenic centers) and make more difficult the chiral amplification.[20] The influence of temperature to achieve homochiral mixtures from TPBAs **1** and **2** was also evaluated. Similarly to OPE-TAs, increasing the temperature to 30 or 40 °C results in a smaller dichroic response for both the pristine chiral components and the mixtures of enantiomers compared to 20 °C (Figure S8). However, the chiral amplification ability exhibited by TPBAs **1**–**2** remains nearly unaltered upon this temperature increase (Figure 3). Indeed, the application of the two-components EQ model to the MRs experiments performed with mix-

Table 2. Mismatch penalty (MMP, in kJ mol^{-1}) derived from fitting the MRs data.[a]

	1a+2a (3*S*+3*R*)	**1b+2b** (2*S*+2*R*)	**1c+2c** (1*S*+1*R*)
MMP 20 °C	1.4 ± 0.1	1.3 ± 0.1	1.6 ± 0.1
MMP 30 °C	1.8 ± 0.1	1.4 ± 0.1	1.6 ± 0.1
MMP 40 °C	2.3 ± 0.3	2.1 ± 0.1	3.1 ± 0.2

[a] All the experiments were performed in MCH/DCE 95:5 at c_T = 10 μM.

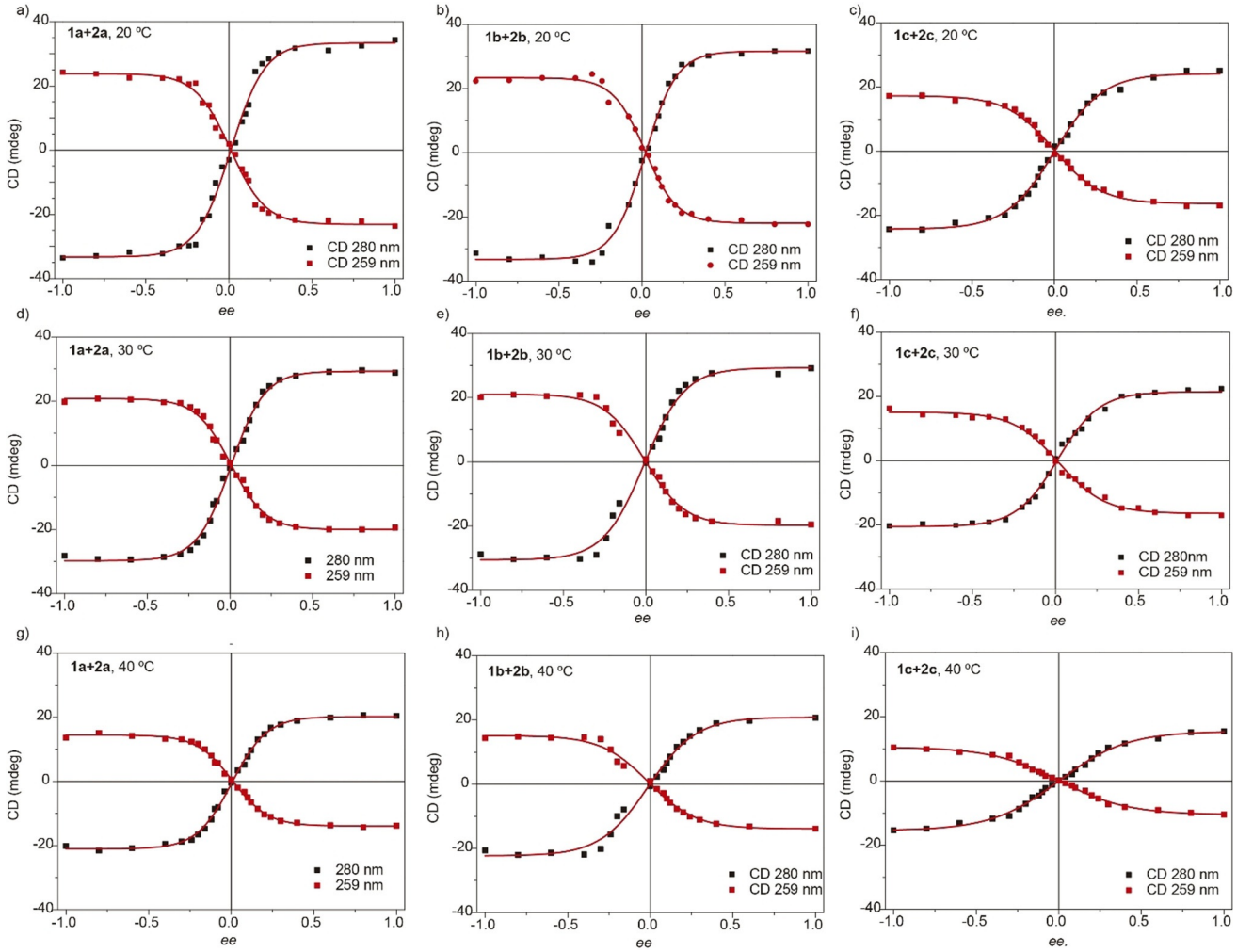

Figure 3. Changes in CD intensity (black squares: $\lambda = 280$ nm, red squares: $\lambda = 259$ m) as a function of *ee* upon adding the enantiomers with (*S*) stereocenters to a solution of the corresponding (*R*) enantiomer (MCH/DCE, 95:5, $c_T = 10$ μM) at 20 °C (a–c), 30 °C (d–f) and 40 °C (g–i). *ee* = 1.0 corresponds to pure (*S*) enantiomers and *ee* = −1.0 corresponds to pure (*R*) enantiomers. The red curves correspond to a sigmoidal fitting to guide the eye.

tures of **1** and **2** at 30/40 °C yields MMP values slightly higher than those derived from experiments at 20 °C (Table 2).

The comparison of the cooling curves obtained for the pristine chiral components with those of the mixtures at different *ee* ratios were previously used in BTAs and OPE-TAs to get a better understanding of the influence of temperature on chiral amplification.[18b,c,20] Figure S10 shows the cooling curves recorded for pure enantiomers of TPBAs **1** and **2** together with those registered for mixtures of these tricarboxamides at two different *ee* ratios. In the case of TPBAs, all the samples, pure enantiomers and mixtures, present a gradual decrease of the dichroic response upon increasing the temperature until reaching the elongation temperature T_e. At this T_e, the dichroic response is cancelled due to the disassembly of the helical columnar stacks into the constitutive monomeric units. This behavior is similar to that observed for OPE-TAs [20] and contrasts with that reported for BTAs, for which the dichroic response increases with temperature and full homochirality is afforded more easily at higher temperatures.[18b,c,20]

Theoretical calculations

To shed light on the chiral amplification ability of TPBAs and to rationalize the differences found for these tricarboxamides in comparison to BTAs and OPE-TAs, the supramolecular aggregates formed by TPBAs **1**–**2** were theoretically investigated. First, the geometries of the symmetric **2a** and the asymmetric **2b** and **2c**, respectively endowed with three, two, and one chiral chains bearing *R*-stereogenic groups, were optimized at the density functional theory (DFT) level using the B3LYP functional,[27] the 6-31G** basis set,[28] and the Grimme's dispersion correction D3.[29] Similarly to the C_3-symmetric TPBAs previously studied,[21] the **2a**–**c** monomeric units exhibit a propeller-like geometry, in which the phenyl rings of the TPB core are twisted by ≈37° (Figure S11). This disposition favors the helical arrangement of the monomeric units by the formation of a triple array of H-bonding interactions between the amide functional groups and the π-stacking of the aromatic TPB moieties.

The optimized monomeric units of **2a**–**c** were taken to build up *P*- and *M*-type helical supramolecular stacks of 20 monomeric units that were fully optimized at the cost-effective

GFN2-xTB level[30] (see the Supporting Information for full computational details). From the optimized helical aggregates, the central dodecamer was extracted to avoid terminal effects and its energy was recalculated in a single-point calculation to get comparable energies. Calculations confirmed the anti-clockwise *M*-type helical handedness as the preferred arrangement for TPBAs **2a**–**c** (Figure 4). For all the three molecules, the most stable oligomer corresponds to the left-handed assembly in which the chiral aliphatic chains in vicinal molecules along the stack are in an eclipsed disposition (Figures S12 and S13). This disposition is found to be 16.5 (**2a**), 6.3 (**2b**) and 1.3 kJ mol^{-1} (**2c**), per monomeric unit, more stable than the respective lowest-energy *P*-type helix (Figure S14). Parallel results are expected for compounds **1a**–**c** bearing *S*-stereogenic centers, for which a clockwise or right-handed *P*-type helical arrangement is preferred.

In the most stable *M*-dodecamers, the separation between the monomeric units slightly depends on the nature of the three appended side chains. The average intermolecular distance between the centroids of the TPB cores along the stack is computed quite similar for **2a**, **2b**, and **2c**, with values of 3.49 ± 0.04, 3.44 ± 0.07, and 3.50 ± 0.04 Å, for three, two and, one chiral chains, respectively. Rotation angles between vicinal molecules along the stack are also calculated very similar upon increasing the number of chiral chains, with average values of 26 ± 2, 26.7 ± 1.7, and 26.4 ± 1.2°, respectively. As a result, comparable H-bond interactions with distances of 1.87 ± 0.08, 1.88 ± 0.08, and 1.85 ± 0.05 Å are obtained in the supramolecular assemblies of **2a**, **2b**, and **2c**, respectively. It should be noted that the helical disorder is more significant in the derivative with only one chiral chain (**2c**), probably due to the higher degree of packing freedom of the achiral side chains (Figure 4). As discussed above, the TPB core displays a propeller-like nonplanar geometry due to the rotation of the benzamide moieties out the plane of the central ring.[21] This geometry weakens the interactions between vicinal monomers compared to fully planar cores, and allows their slipping along the stacking axis of polymerization leading to ill-defined helical structures (see Figure S13). Indeed, the distance between the centroids of the central benzene rings and the stacking axis are in the range of 0.82–1.47 Å for **2a** and widens to 0.56–1.76 Å for **2c** (Table S1). The tilting angle of the central benzene rings with respect to the stacking axis also exhibits a wider dispersion for **2c** (57–73°) than for **2a** (57–63°). Chiral side chains therefore favor order in the resulting supramolecular aggregate by reducing the flexibility of the alkyl chains, and induce a unique helical orientation of the assembly through discrete alkyl–alkyl interactions between the branching groups. The proximity of the stereogenic groups to the central aromatic core forces a more rigid helical structure in **2a** and **2b** compared to that optimized for **2c** with more flexible linear achiral chains.

Theoretical calculations were then performed to investigate the chiral amplification ability of TPBAs in comparison to their referable congeners BTAs and OPE-TAs. Theoretical simulations of majority rules experiments were carried out by replacing one central (*R*)-chiral TPBA in the left-handed *M*-helix stack of the 20-mer by the corresponding "wrong" (*S*)-chiral TPBA. The resulting 20-mer was fully optimized at the GFN2-xTB level, and the central dodecamer was extracted and single-point recalculated (see the Supporting Information for full computational details). Theoretical calculations predict similar MMP values of 0.63, 0.51, and 1.02 kJ mol^{-1} for **2a**, **2b**, and **2c**, respectively. This energy penalty corresponds to the difference between the total energy calculated for the central 12-mer incorporating one "wrong" (*S*)-chiral monomer and the energy of the regular 12-(*R*)-mer divided by the number of monomers (i.e., 12). Although slightly smaller, the theoretical MMP values nicely agree with the experimental trends (Table 2). Therefore, and in contrast to BTAs and OPE-TAs, TPBAs shows similar MMP values irrespective of the number of chiral chains in the monomer.

The mismatch penalty can be understood as the energy increase provoked by the steric hindrance when a chiral molecule is introduced in an aggregate of its unpreferred helicity. The lower MMP values obtained for TPBAs compared to OPE-TAs and BTAs may be explained from the lower steric hindrance between peripheral chiral chains due to longer (more alleviated) intermolecular contacts (Figure 5). TPBAs present a rotational angle of around 26° and the intermolecular contacts are similar (i.e., comparable steric hindrance), independently of the number of chiral aliphatic chains in the monomer, which keeps the MMP mainly unaltered. OPE-TAs exhibit a smaller torsion angle of ca. 18°,[20] and therefore the penalty exerted by the steric hindrance is expected to be higher due to shorter alkyl-alkyl contacts. This rationale is supported by the C–H···H–C distances between side chains in adjacent molecules, with shortest values around 3.35 Å for OPE-TAs and 4.25 Å for TBPAs. Otherwise, BTAs present larger rotation angles of ca.

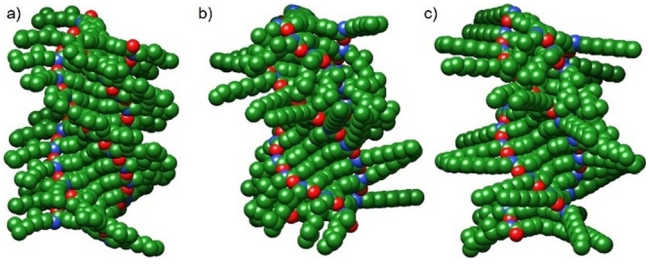

Figure 4. Representation of the most-stable dodecamers (*M*-type) of compounds **2a** (a), **2b** (b), and **2c** (c). Hydrogen atoms are omitted for clarity.

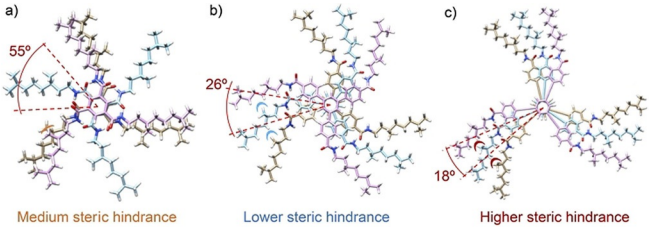

Figure 5. Schematic illustration of the steric hindrance effect exerted by the chiral aliphatic chains of vicinal units in BTAs (a), TPBAs (b) and OPE-TAs (c).

55°, with significantly longer chain-to-chain distances, in the range of 5.8–6.5 Å.[20] However, second neighbors in BTAs are almost perfectly stacked, with distances between side chains of around 4.0 Å, slightly shorter than those calculated for TPBAs. Intermolecular chain-to-chain contacts may therefore explain the origin of the smaller mismatch penalties obtained for TBPAs.

As stated above, the CD spectra of TPBAs **1c** and **2c** exhibit a strong contamination due to LD effects. In our previous study on C_3-symmetric TPBAs, we investigated the bundling effect favored by van der Waals interactions between the peripheral aliphatic chains of vicinal helical aggregates in achiral **3** and fully chiral **1a**/**2a** derivatives.[21] Herein, we extend the study of bundle formation to asymmetric TPBAs **2b** and **2c**. Figure 6 displays the bundles formed by two interdigitated icosamers of these TPBAs, where the helical rotation axes of the two columnar aggregates are mainly parallel. The structure of the bundle was fully optimized at the molecular mechanics level (see the Supporting Information for computational details).

For **2b**, the two aggregates are separated by 31.5 Å and present an intercolumnar interaction energy ($E_{int,col}$) of $-126\ kJ\,mol^{-1}$. For **2c**, the distance between the helices is shorter (30.0 Å) and the $E_{int,col}$ is calculated to be significantly larger ($-276\ kJ\,mol^{-1}$). The bundle structures calculated for **2b** and **2c** actually constitute intermediate situations between that computed for fully chiral **2a** (32.4 Å, $-98\ kJ\,mol^{-1}$) and achiral **3** (29.1 Å, $-373\ kJ\,mol^{-1}$) derivatives (Figure S16 and Table S2). The larger helix-to-helix interaction energy and the slightly shorter intercolumnar distance obtained along the series **2a**–**2b**–**2c**–**3** can be justified by the smaller number of branched, chiral side chains, which enhances a more efficient bundling effect between the columnar aggregates. The values obtained for **2b** are indeed similar to those of **2a** and significantly different from those predicted for **2c** and achiral **3**, thus explaining the LD effects experimentally observed for the latter.

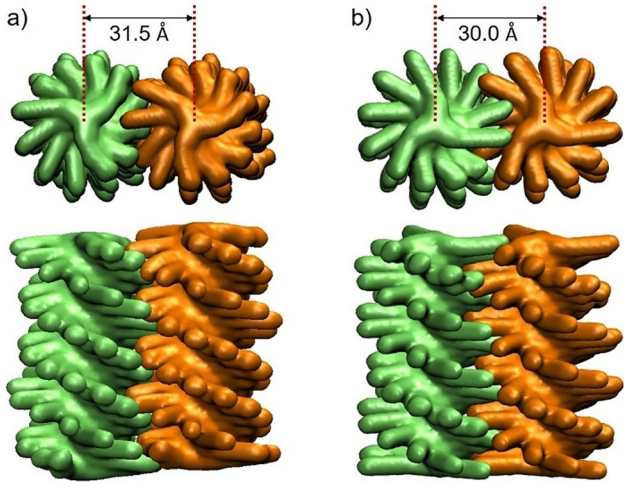

Figure 6. Top and side views of the surface representation of the homochiral helix-to-helix interaction of TPBAs **2b** (a) and **2c** (b). The distance between the two column centers is indicated in the top view.

Conclusions

Herein, we report on a detailed investigation of the chiral amplification ability exhibited by 1,3,5-triphenylbenzene-tricarboxamides (TPBAs) in comparison to the closely referable BTA and OPE-TA tricarboxamides by doing majority rules experiments. As previously observed for the latter, the decoration of TPBAs with three, two or one chiral side chains bearing stereogenic centers results in a similar dichroic response. This indicates that only one chiral chain is enough to achieve an efficient transfer of the point chirality embedded in the chains to the supramolecular chirality associated to the formation of helical aggregates. However, the chiral amplification ability of TPBAs differs from that reported for BTAs and OPE-TAs. In BTAs, the chiral amplification ability increases by decreasing the number of stereogenic centers per monomeric unit, the trend being opposite for OPE-TAs in which the larger the number of stereogenic centers, the lower the chiral amplification ability. In contrast, the chiral amplification of TPBAs exhibits almost no dependence on the number of chiral centers per monomeric unit, and stands the largest among the series of tricarboxamides. Theoretical studies demonstrate that the rotation angle between the TPBAs units in the helical stack is intermediate to that observed for BTAs and OPE-TAs, and strongly conditions the steric interactions between vicinal molecules in the stack and the final chiral amplification outcome. Theoretical calculations furthermore show that achiral side chains favor the interdigitation of the helical aggregates and thereby the formation of bundle superstructures, which justifies the experimentally observed LD effect. The results presented in this work confirm the strong dependence of the chiral amplification ability of self-assembling units on structural factors, like shape and size, and contribute to establish a clear structure–function relationship in chiral supramolecular co-polymers.

Acknowledgements

Financial support by the MICINN of Spain (CTQ2017-82706-P, PGC2018-099568-B-I00, RED2018-102331-T and Unidad de Excelencia María de Maeztu MDM-2015-0538), the Generalitat Valenciana (PROMETEO/2020/077 and SEJI/2018/035), the Comunidad de Madrid (NanoBIOCARGO, S2018/NMT-4389), and European FEDER funds (PGC2018-099568-B-I00) is acknowledged. Y.D. is grateful to the Comunidad de Madrid for his predoctoral fellowship. J.C. and J.A. are grateful to MICINN for a predoctoral contract and a "Ramon-y-Cajal" fellowship (RyC-2017–23500), respectively.

Conflict of interest

The authors declare no conflict of interest.

Keywords: C_3-symmetric molecules · chiral amplification · helicity · supramolecular polymers · theoretical calculations

[1] a) W. A. Bonner, *Origins Life Evol. Biospheres* **1991**, *21*, 59 – 111; b) B. L. Feringa, R. A. van Delden, *Angew. Chem. Int. Ed.* **1999**, *38*, 3418 – 3438; *Angew. Chem.* **1999**, *111*, 3624 – 3645; c) I. Weissbuch, L. Leiserowitz, M. Lahav, *Top. Curr. Chem.* **2005**, *259*, 123 – 165.
[2] M. M. Green, M. P. Reidy, R. J. Johnson, G. Darling, D. J. O'leary, G. Willson, *J. Am. Chem. Soc.* **1989**, *111*, 6452 – 6454.
[3] M. M. Green, B. A. Garetz, B. Muñoz, H. Chang, S. Hoke, R. G. Cooks, *J. Am. Chem. Soc.* **1995**, *117*, 4181 – 4182.
[4] a) M. Raynal, F. Portier, P. W. N. M. van Leeuwen, L. Bouteiller, *J. Am. Chem. Soc.* **2013**, *135*, 17687 – 17690; b) Y.-Z. Ke, Y. Nagata, T. Yamada, M. Suginome, *Angew. Chem. Int. Ed.* **2015**, *54*, 9333 – 9337; *Angew. Chem.* **2015**, *127*, 9465 – 9469; c) A. Desmarchelier, X. Caumes, M. Raynal, A. Vidal-Ferran, P. W. N. M. van Leeuwen, L. Bouteiller, *J. Am. Chem. Soc.* **2016**, *138*, 4908 – 4916; d) Y. Li, A. Hammoud, L. Bouteiller, M. Raynal, *J. Am. Chem. Soc.* **2020**, *142*, 5676 – 5688.
[5] a) J. H. Jung, S.-J. Moon, J. Ahn, J. Jaworski, S. Shinkai, *ACS Nano* **2013**, *7*, 2595 – 2601; b) H. Cao, X. Zhu, M. Liu, *Angew. Chem. Int. Ed.* **2013**, *52*, 4122 – 4126; *Angew. Chem.* **2013**, *125*, 4216 – 4220; c) Y. Fang, E. Ghijsens, O. Ivasenko, H. Cao, A. Noguchi, K. S. Mali, K. Tahara, Y. Tobe, S. De Feyter, *Nat. Chem.* **2016**, *8*, 711 – 717.
[6] a) B. Nieto-Ortega, F. García, G. Longhi, E. Castiglioni, J. Calbo, S. Abbate, J. T. López Navarrete, F. J. Ramírez, E. Ortí, L. Sánchez, J. Casado, *Chem. Commun.* **2015**, *51*, 9781 – 9784; b) T. Ikai, S. Shimizu, S. Awata, K. Shinohara, *Macromolecules* **2018**, *51*, 2328 – 2334; c) E. E. Greciano, R. Rodríguez, K. Maeda, L. Sánchez, *Chem. Commun.* **2020**, *56*, 2244 – 2247.
[7] a) A. R. A. Palmans, E. W. Meijer, *Angew. Chem. Int. Ed.* **2007**, *46*, 8948 – 8968; *Angew. Chem.* **2007**, *119*, 9106 – 9126; b) Y. Dorca, E. E. Greciano, J. S. Valera, R. Gómez, L. Sánchez, *Chem. Eur. J.* **2019**, *25*, 5848 – 5864.
[8] a) A. Lohr, F. Würthner, *Angew. Chem. Int. Ed.* **2008**, *47*, 1232 – 1236; *Angew. Chem.* **2008**, *120*, 1252 – 1256; b) A. Lohr, F. Würthner, *Chem. Commun.* **2008**, 2227 – 2229.
[9] a) G. Ghosh, M. Paul, T. Sakurai, W. Matsuda, S. Seki, S. Ghosh, *Chem. Eur. J.* **2018**, *24*, 1938 – 1946; b) S. Ghosh, X.-Q. Li, V. Stepanenko, F. Würthner, *Chem. Eur. J.* **2008**, *14*, 11343 – 11357.
[10] a) T. Kaiser, V. Stepanenko, F. Würthner, *J. Am. Chem. Soc.* **2009**, *131*, 6719 – 6732; b) T. Seki, A. Asano, S. Seki, Y. Kikkawa, H. Murayama, T. Karatsu, A. Kitamura, S. Yagai, *Chem. Eur. J.* **2011**, *17*, 3598 – 3608.
[11] a) A. Ajayaghosh, R. Varghese, S. J. George, C. Vijayakumar, *Angew. Chem. Int. Ed.* **2006**, *45*, 1141 – 1144; *Angew. Chem.* **2006**, *118*, 1159 – 1162; b) A. Ajayaghosh, R. Varghese, S. Mahesh, V. K. Praveen, *Angew. Chem. Int. Ed.* **2006**, *45*, 7729 – 7732; *Angew. Chem.* **2006**, *118*, 7893 – 7896; c) C. Kulkarni, R. Munirathinam, S. J. George, *Chem. Eur. J.* **2013**, *19*, 11270 – 11278; d) P. A. Korevaar, C. Grenier, A. J. Markvoort, A. P. H. J. Schenning, T. F. A. de Greef, E. W. Meijer, *Proc. Natl. Acad. Sci. USA* **2013**, *110*, 17205 – 17210; e) F. Aparicio, B. Nieto-Ortega, F. Nájera, F. J. Ramírez, J. T. López Navarrete, J. Casado, L. Sánchez, *Angew. Chem. Int. Ed.* **2014**, *53*, 1373 – 1377; *Angew. Chem.* **2014**, *126*, 1397 – 1401; f) S. C. Karunakaran, B. J. Cafferty, A. Weigert-Muñoz, G. B. Schuster, N. V. Hud, *Angew. Chem. Int. Ed.* **2019**, *58*, 1453 – 1457; *Angew. Chem.* **2019**, *131*, 1467 – 1471.
[12] Y. Dorca, J. Matern, G. Fernández, L. Sánchez, *Isr. J. Chem.* **2019**, *59*, 869 – 880.
[13] a) A. T. Haedler, S. C. J. Meskers, R. H. Zha, M. Kivala, H.-W. Schmidt, E. W. Meijer, *J. Am. Chem. Soc.* **2016**, *138*, 10539 – 11545; b) T. Kim, T. Mori, T. Aida, D. Miyajima, *Chem. Sci.* **2016**, *7*, 6689 – 6694; c) J. S. Valera, R. Gómez, L. Sánchez, *Small* **2018**, *14*, 1702437; d) J. S. Valera, R. Gómez, L. Sánchez, *Angew. Chem. Int. Ed.* **2019**, *58*, 510 – 514; *Angew. Chem.* **2019**, *131*, 520 – 524; e) M. A. J. Koenis, A. Osypenko, G. Fuks, N. Giuseppone, V. P. Nicu, L. Visscher, W. J. Buma, *J. Am. Chem. Soc.* **2020**, *142*, 1020 – 1028.
[14] T. F. A. de Greef, M. M. J. Smulders, M. Wolffs, A. P. H. J. Schenning, R. P. Sijbesma, E. W. Meijer, *Chem. Rev.* **2009**, *109*, 5687 – 5754.
[15] a) H. M. M. ten Eikelder, A. J. Markvoort, T. F. A. de Greef, P. A. J. Hilbers, *J. Phys. Chem. B* **2012**, *116*, 5291 – 5301; b) H. M. M. ten Eikelder, B. Adelizzi, A. R. A. Palmans, A. J. Markvoort, *J. Phys. Chem. B* **2019**, *123*, 6627 – 6642.
[16] a) B. Adelizzi, N. J. Van Zee, L. N. J. de Windt, A. R. A. Palmans, E. W. Meijer, *J. Am. Chem. Soc.* **2019**, *141*, 6110 – 6121; b) H. M. M. ten Eikelder, A. J. Markvoort, *Acc. Chem. Res.* **2019**, *52*, 3465 – 3474.
[17] J. van Gestel, *Macromolecules* **2004**, *37*, 3894 – 3898.
[18] a) J. van Gestel, A. R. A. Palmans, B. Titulaer, J. A. J. M. Vekemans, E. W. Meijer, *J. Am. Chem. Soc.* **2005**, *127*, 5490 – 5494; b) M. M. J. Smulders, I. A. W. Filot, J. M. A. Leenders, P. van der Schoot, A. R. A. Palmans, A. P. H. J. Schenning, E. W. Meijer, *J. Am. Chem. Soc.* **2010**, *132*, 611 – 619; c) M. M. J. Smulders, P. J. M. Stals, T. Mes, T. F. E. Paffen, A. P. H. J. Schenning, A. R. A. Palmans, E. W. Meijer, *J. Am. Chem. Soc.* **2010**, *132*, 620 – 626; d) A. J. Markvoort, H. M. M. ten Eikelder, P. A. J. Hilbers, T. F. A. de Greef, E. W. Meijer, *Nat. Commun.* **2011**, *2*, 509; e) F. García, P. A. Korevaar, A. Verlee, E. W. Meijer, A. R. A. Palmans, L. Sánchez, *Chem. Commun.* **2013**, *49*, 8674 – 8676.
[19] B. Jouvelet, B. Isare, L. Bouteiller, P. van der Schoot, *Langmuir* **2014**, *30*, 4570 – 4575.
[20] E. E. Greciano, J. Calbo, J. Buendía, J. Cerdá, J. Aragó, E. Ortí, L. Sánchez, *J. Am. Chem. Soc.* **2019**, *141*, 7463 – 7472.
[21] S. Díaz-Cabrera, Y. Dorca, J. Calbo, J. Aragó, R. Gómez, E. Ortí, L. Sánchez, *Chem. Eur. J.* **2018**, *24*, 2826 – 2831.
[22] a) A. Tsuda, M. D. Alam, T. Harada, T. Yamaguchi, N. Ishii, T. Aida, *Angew. Chem. Int. Ed.* **2007**, *46*, 8198 – 8202; *Angew. Chem.* **2007**, *119*, 8346 – 8350; b) M. Wolffs, S. J. George, Z. Tomovic, S. C. J. Meskers, A. P. H. J. Schenning, E. W. Meijer, *Angew. Chem. Int. Ed.* **2007**, *46*, 8203 – 8205; *Angew. Chem.* **2007**, *119*, 8351 – 8353; c) J. Buendía, J. Calbo, E. Ortí, L. Sánchez, *Small* **2017**, *13*, 1603880.
[23] TPBAs are sparingly soluble in pristine MCH even at high dilutions. Therefore, the addition of a good co-solvent is required to achieve homogenous solutions of the aggregated and monomeric species of the reported TPBAs.
[24] a) E. E. Greciano, S. Alsina, G. Gosh, G. Fernández, L. Sánchez, *Small Methods* **2020**, *4*, 1900715; b) M. Wehner, M. I. S. Röhr, M. Bühler, V. Stepanenko, W. Wagner, F. Würthner, *J. Am. Chem. Soc.* **2019**, *141*, 6092 – 6107; c) D. S. Philips, K. K. Kartha, A. T. Politi, T. Krügger, R. Q. Albuquerque, G. Fernández, *Angew. Chem. Int. Ed.* **2019**, *58*, 4732 – 4736; *Angew. Chem.* **2019**, *131*, 4782 – 4787.
[25] F. C. Spano, *Acc. Chem. Res.* **2010**, *43*, 429 – 439.
[26] a) N. Harada, K. Nakanishi, *J. Am. Chem. Soc.* **1969**, *91*, 3989 – 3991; b) F. García, P. M. Viruela, E. Matesanz, E. Ortí, L. Sánchez, *Chem. Eur. J.* **2011**, *17*, 7755 – 7759; c) F. García, L. Sánchez, *J. Am. Chem. Soc.* **2012**, *134*, 734 – 742.
[27] a) C. Lee, W. Yang, R. G. Parr, *Phys. Rev. B* **1988**, *37*, 785 – 789; b) A. D. Becke, *J. Chem. Phys.* **1993**, *98*, 5648 – 5652.
[28] M. M. Francl, W. J. Pietro, W. J. Hehre, J. S. Binkley, M. S. Gordon, D. J. DeFrees, J. A. Pople, *J. Chem. Phys.* **1982**, *77*, 3654 – 3665.
[29] a) S. Grimme, J. Antony, S. Ehrlich, H. Krieg, *J. Chem. Phys.* **2010**, *132*, 154104; b) S. Grimme, S. Ehrlich, L. Goerigk, *J. Comput. Chem.* **2011**, *32*, 1456 – 1465.
[30] C. Bannwarth, S. Ehlert, S. Grimme, *J. Chem. Theory Comput.* **2019**, *15*, 1652 – 1671.

Manuscript received: June 15, 2020
Accepted manuscript online: July 28, 2020
Version of record online: October 9, 2020